Application of Quasi-PSI method for landslide determination in Northern mountainous region of Vietnam by multi sensor Radar satellite images

Van Anh TRAN, Quoc Cuong TRAN, An Binh NGUYEN, Trung Anh TRAN, Vietnam

Key words: Landslide, Quasi-PSI, Sentinel-1A, ALOS PalSAR-1

SUMMARY

Radar technology recently has been applying for many researches relating to terrain changes such as landslides, land subsidence with several methods of interferometry SAR radar (InSAR) such as: DInSAR, PSInSAR, SqueerSAR. Each method has different characteristics and advantages, but for mountainous Vietnam with high coverage of vegetation, humidity and cloudy, DInSAR method is limited due to atmospheric influences. The PSInSAR method eliminates this disadvantage of DInSAR by using a series of images and only determines the permanent scattering points, which are the points in all pairs of images with high coherence. However, one drawback of traditional PSInSAR is that it only determines linear land deformations while nonlinear deformations are less accurate. In this paper, we used an improved PSInSAR method called Quasi-PSI. This method does not use one master image and the other one are the slave images like traditional PSInSAR but uses multiple master images to connect both images of the dataset to multiple pairs of images that make up the minimum spanning tree chart. The study area was part of Bat Xat district and part of Sa Pa district in Lao Cai province with an area of 20kmx20 km. The images were used as a series of 13 ALOS PalSAR-1 scenes from 2007 to 2010 and 18 Sentinel 1A scenes from March 2017 to July 2018. The landslide location was determined from the satellite images that were concentrated mostly near rivers, streams and roads in communes such as Den Sang, Bat Xat district and Ta Phin communes, Sa Pa town, Sa Pa district. The landslide determination results have been compared with the surveying landslides provided by the Vietnam Institute of Geosciences and Mineral Resources and have proven its ability to detect landslides by the ALOS PalSAR images and Sentinel-1A images for the mountainous areas which have large landslide phenomenon.

Application of Quasi-PSI method for landslide determination in Northern mountainous region of Vietnam by multi sensor Radar satellite images

Van Anh TRAN, Quoc Cuong TRAN, An Binh NGUYEN, Trung Anh TRAN, Vietnam

1. INTRODUCTION

Landslide is a type of disaster that occurs frequently in mountainous areas of Vietnam, causing severe damage to human lives, material facilities and serious environmental impacts. According to research by the Vietnam Institute of Geosciences and Mineral Resources (Ministry of Natural Resources and Environment): Landslide triggered by many exogenous factors such as rain, storms, floods, soil weathering processes ... and endogenous activities as Earthquake or volcano eruption. Particularly because of the human affecting making the loss of slope stabilization, vibration from landmines or machinery, heavy load on the slope and erosion, the weakening of rocky soil, forest clear-cut, mineral mining, leveling, cutting hills and slopes to build roads, houses and other structures. This leads to landslides and mudslides which have been causing great human and social disasters. Previously, the identification of landslides is often a field survey or use of aerial photographs with visual interpretation. A number of studies using aerial photographs to determine landslides in steep areas have been reported in (Soeters and Westen, 1996). This technique, although able to identify large-scale terrain changes, and coupled with using DEM to find elevation variation, however, it does not automatically in determining the progress of landslides over time. In addition, optical satellite imagery recorded in Asia is often clouded, and in the time of severe change in terrain, it is not always possible to obtain an optical image with good quality.

Therefore, the determination of terrain deformations using Radar satellite images is an option nowadays. Radar satellite images are not affected by clouds and rain and are recorded all day and night, so it is suitable for Southeast Asia, including Vietnam. The technology uses Radar images to identify terrain changes such as landslide, land subsidence is Interferometry SAR methods (InSAR). There are many InSAR methods that scientists have studied and used in the last 20 years: DInSAR (Gabriel and Goldstein, 1989), PSInSAR (Ferretti et al., 2000) or StaMPS (A. Hopper et al. 2012). Since then there have been many studies using those methods to identify landslides such as Bruckno B. et al., (2013); Ran N. Nof et al, (2013); Theron A., et al. (2016); Engelbrecht J., (2016); Kim J.W. et al, (2016) succeeded in early detection and monitoring of soil deformation before slumps appeared on the land surface. The satellite radar data used includes ALOS- PalSAR, COSMO-Sky med, TerraSAR-X, Sentinel 1A.

Each InSAR method has its advantages and disadvantages in determining terrain deformation. For DInSAR the advantage is that the number of images needed in the terrain change study does not require much, just need two images before and after the deformation, but one drawback is that atmospheric influences will produce noise adds to the phase of change that makes the results less accurate. The PSInSAR method can replace DInSAR to determine terrain displacement because it uses a series of images can remove the atmospheric effect but it is difficult to determine landslides or changes in terrain that occur linearly. So in this paper we use an improved approach from PSInSAR called Quasi-PSI developed by Daniel Perissin of the Geoinformatics Lab of Purdue University. The method selected some images to make the master images combine with other slave images in the sequence to optimize the correlation values for the pairs of images.

Our study area is in Lao Cai province, the scene covers part of Bat Xat and Sa Pa districts where there are many landslides on 4D highway or in some communes such as Phin Ngan, Quang Kim, Ta Phin and Sa Pa. The selected images for this study are ALOS PalSAR-1 L band and Sentinel-1A C band.

2. RESEARCH METHOD

According to complex image theory, the interferometric phase of a image pair of two complex images s_i and s_j is determined by multiplying the first complex image with the complex conjugate of the second image with the formula: Ii,j=si.sj* (D. Perissin et al, 2012).

The Quasi-PSI method is a method developed from traditional method of determining ground deformation named DInSAR (Differential SAR Interferometry). This method determines the land deformation by the phase shift between two or three images acquired in different times over the same area on the surface which is called differential interferometry (Fig.1). The equation (1) illustrates the phase of land deformation (Tran Van Anh et al, 2016). Taking the objective P_0 as the reference point, the interferometric phase of the target pij is equal to $\Delta\phi^{i,j}$ depending on its geometry as well as the movement of the object, atmospheric disturbance. In particular, the interferometric phase depends on the height of the target P.

$$\Delta\phi_{P}^{i,j} = \Delta\phi_{D(p,p0)} + \Delta\phi_{H(p,p0)} + \Delta\phi_{ATm(i,j)} + \Delta\phi_{Orb(i,j)} + \phi_{Noise)} \quad (1)$$

$$\Delta\phi_{H,p,po}^{i,j} = \frac{4\pi}{\lambda}\frac{1}{R\sin\theta}\Delta h_{p,po}\, Bn_{i,j} \quad (2)$$

$$\Delta\phi_{D,p,po}^{i,j} = \frac{4\pi}{\lambda}\Delta\nu_{p,po}\, Bt_{i,j} \quad (3)$$

where $\Delta\phi_{P}^{i,j}$ is the interferometric phase of the target Pij of two images S_i and S_j

$\Delta\phi_{D(p,p0)}$ is the deformation phase

$\Delta\phi_{H(p,p0)}$ is the elevation phase

$\Delta\phi_{ATm(i,j)}$ is the atmospheric phase component at different acquisition's times,

$\Delta\phi_{Orb(i,j)}$ is the phase component due to the orbital errors of each image (errors that affect the position of M and S in (Fig. 1)

$\phi_{(Noise)}$ is the phase noise

$\Delta H_{p,p0}$ is the height of point P compared to the reference point P_0

$\Delta\nu_{p,p0}$ is the linear deformation

$Bn_{i,j}$ is the standard baseline of the interferometric pair

$Bt_{i,j}$ is the time-baseline of the image pairs, λ is the wavelength, θ is the looking angle and R the sensor-target distance. Within the PS technique, the target height and velocity are estimated by maximizing ξp (P_0 in the equation is removed to lighten the notation):

$$\left(\Delta\hat{h}_p, \Delta\hat{\nu}_p\right) = \arg\{\max(|\xi_p|)\} \quad (4)$$

$$\xi_p = \frac{\sum_{i=1}^{N} e^{j(\Delta\phi_{P}^{i,j} - \Delta\bar{\phi}_{H,p}^{i,j} - \Delta\bar{\phi}_{D,p}^{i,j}}}{N} \quad (5)$$

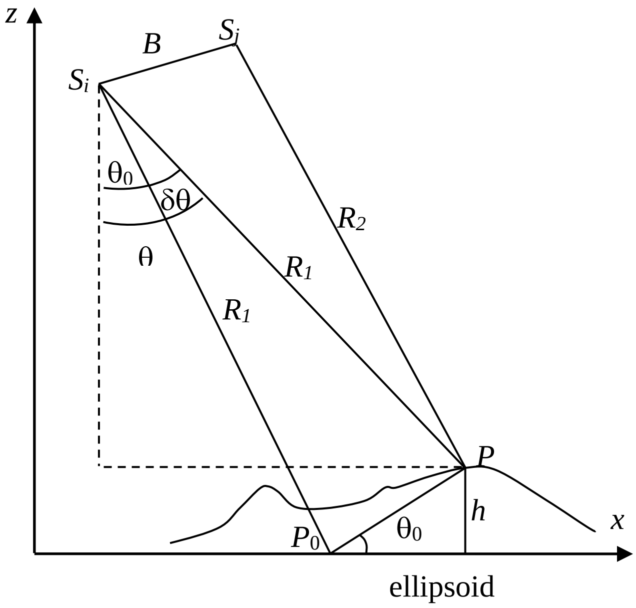

Figure 1: The principle of Interferometry SAR

In Eq. 5 the following terms can be highlighted:

- $\Delta\overline{\phi}^{i,j}_{H,p}$ is the elevation-dependent term given by Eq. 2;
- $\Delta\overline{\phi}^{i,j}_{D,p}$ is the deformation trend-dependent term given by Eq. 3

In classical PS analysis, the interferometric phase in equation (5) is created by taking a master image and all remaining images are slave images. In the standard base line and the distance from the standard baseline time, this configuration can be represented by a star chart, where each point represents an image position and each connection is the interferometric pair in the sample data set. The main disadvantage of this combination is that each image can create an interferogram with the master image without knowing whether the combination is good or not. Other improvements to eliminate the limitation of the use of one master image are: (SBAS (Berardino, 2002) or StamPS (Hooper, A, 2004)). Yet in this study we applied Quasi-PSI method of D.Perisin (D.Perissin et al, 2012) which searched the minimum best coherent graph connecting all the images of the data-set (commonly known as the Minimum Spanning Tree, MST (Refice A, 2003)), without impose any pre-defined decorrelation model.

To achieve this goal with a limited computational cost, each graph connection i, j was assigned to the absolute value of the spatial correlation $\gamma^{i,j}_{p}$ on a set of given points. Then we searched among the N(N-1)/2 possible interferograms for the MST that maximizes the average coherence. The spatial coherence $\gamma^{i,j}_{p}$ of point p is retrieved as the normalized cross-correlation coefficient between images i,j over an appropriate neighbourhood Win(p) of p

$$\gamma^{i,j}_{p} = \frac{\sum_{Win(p)} S_i S_j^*}{\sqrt{\sum_{Win(p)} |S_i|^2 \sum_{Win(p)} |S_j|^2}} \qquad (6)$$

Regardless of the selected graph, the set of coherent interferograms that carry information can be different from point to point. Again, only PS's are coherent in all interferograms. Thus, in order to estimate height and deformation trend also of partially coherent targets, a sub-set of coherent interferograms have been chosen for each point. To this purpose we can exploit the absolute value of the spatial coherence $\gamma_p^{i,j}$ of point p. By inserting it as a weight in the estimation process, only coherent interferograms will determine the result. Eq. 5 becomes equation (7) (D. Perissin et al, 2012):

$$\xi_p = \frac{\sum_{(i,j)} \left|\gamma_p^{i,j}\right| e^{j(\Delta\phi_p^{i,j} - \Delta\bar{\phi}_{H,p}^{i,j} - \Delta\bar{\phi}_{D,p}^{i,j})}}{\sum_{(i,j)} \left|\gamma_p^{i,j}\right|} \qquad (7)$$

As far as we have mentioned, the Quasi-PSI method is also completely based on the phase difference to create the interferogram, then the terrain deformation can be extracted (Eq. 1). However, the task of the Quasi-PSI method here is to select the coherent interferograms of the pixels on the time series which satisfy Eq.7. Since then, this coefficient can be used as a weight for determining the permanent scatter points (PS). For more detail about the Quasi PSI method, you can refer the paper about interferometry with partially coherent targets (D. Perissin et al, 2012).

3. STUDY AREA AND DATA USAGE

3.1. Study area

The northern mountainous of Vietnam includes provinces adjacent to China such as Cao Bang, Lang son, Ha Giang, Lao Cai, Dien Bien, Lai Chau and Quang Ninh. This mountainous area consists of plateaus from west to east: Bac Ha plateau, Quan Ba plateau and Dong Van plateau. The first two plateaus have an average height of 1000–1200 m. Dong Van plateau is 1600 m high. Rivers and streams flow through the plateau to create some long and deep gorges. In the northwest, there is the Hoang Lien Son mountain range extends 180 km from northwest to southeast, between Lao Cai and Lai Chau provinces, continuing to the west of Yen Bai province. This is the end of the Ai Lao Son mountain range (from China), the southeastern end of the Himalayan mountain range. The northwestern part of the Hoang Lien Son contains many high mountains above 2800 m, including the Fan Xi Pang peak of 3143 m (Le Ba Thao 2009).

This area has experienced a lot of landslides in recent years affecting people's lives. In which provinces such as Lao Cai, Ha Giang and Lai Chau are hot spots that often happen landslides after heavy rains. Due to the large coverage of northern mountainous, we selected an area with a lot of landslides, some of them in Sapa and Bat xat districts, Laocai province (Fig. 2).

The entire terrain of this area is formed by many high mountain ranges, highlighting the two main mountain ranges forming the watersheds: Ngoi Phat, Lung Po stream, Quang Kim stream. Terrain changes gradually, the highest point with an elevation of 2945m, the lowest point with an elevation of 88m.

Bat Xat and Sa Pa topography formed two areas: high mountains with high division, narrow valley deep slope, large slope. The lowland is the place where the low hills, relatively flat terrain is concentrated. Every year from July to September is a period of high rainfall and frequent landslide and flash floods in mountainous areas of Vietnam, of which Bat Xat district includes Phin Ngan, Quang Kim, or district Sa Pa in Ta Phin, Trung Chai and Khoang communes are hot spots of landslide. The area covered by the study area is overlaid with the administrative boundary map.

(a) 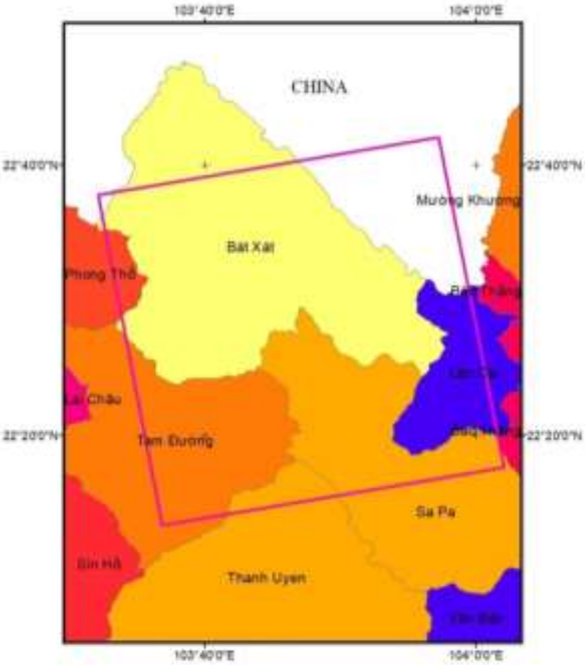

(b) 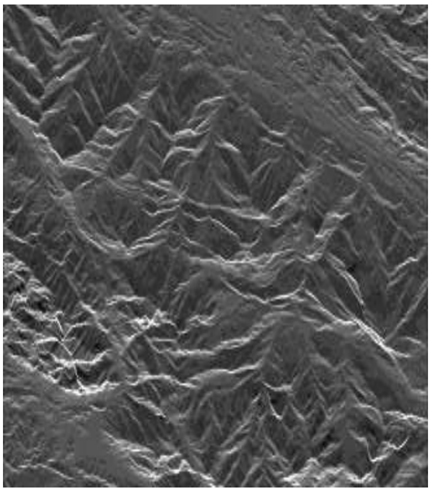

Figure 2: (a): The study area frame was overlapped with the administrative boundary map, (b): The study area image was cut from the Sentinel-1A image acquired on July 30, 2018

3.2. Data usage

In this study we focus on the use of free images such as ALOS PalSAR-1 and Sentinel-1A. Two types of radar satellite images were acquired at different times of 2007-2010 and 2017-2018 because the ALOS PalSAR -1 image began to be recorded from 2006 and ended in 2011. We have exploited all of images in the Alaska Satellite Facility (ASF) database of Laocai area. For the Sentinel-1A, this kind of image was acquired from 2014, but in Laocai area, the images from 2014 were very few and different mode therefore there were only 18 images in the archives that were selected.

In case of ALOS PALSAR, 13 ascending images with 16m spatial resolution were used. The image dataset covered the path of 478, and two frames 440, 430 constitute the data stack during a time span of three years, from August 2007 to November 2010. Table 1 shows the dataset of ALOS PalSAR informations. These PALSAR level 1.1 data consists dual polarization mode (FBD) are processed to chose HH polarization. Beside that 18 Sentinel -1A band C with ascending orbit, spatial resolution in both directions range and azimuth directions respectively 2.3m and 13.9m were processed. The image dataset with the path of 26 and a frame of 68 constitutes the data set for a two-year period, from March 2017 to July 2018. Table 1 is also a data aggregation information of the Sentinel -1A. Data were processed at level 1.1 in dual polarized mode (FBD) to select the VV polarization. Besides, the SRTM digital elevation model (DEM) with a resolution of 90 m was used to remove the topography and correction of geographic coordinates of the Vietnamese region.

Table 1: Parameters of the ALOS PalSAR and Sentinel-1A images in Batxat-Sapa area

ALOS PalSAR				Sentinel -1A			
No	Date of Acquisition	Polarization	Orbit	No	Date of Acquisition	Polarization	Orbit
1	2007/08/10	HH	Ascending	3	2017/04/30	VV	Ascending
2	2007/09/25	HH	Ascending	4	2017/05/24	VV	Ascending
3	2007/11/10	HH	Ascending	5	2017/08/04	VV	Ascending
4	2008/05/12	HH	Ascending	6	2017/08/16	VV	Ascending
5	2008/06/27	HH	Ascending	7	2017/09/21	VV	Ascending
6	2008/08/12	HH	Ascending	8	2017/10/15	VV	Ascending
7	2009/06/30	HH	Ascending	9	2017/10/27	VV	Ascending
8	2009/08/15	HH	Ascending	10	2017/11/20	VV	Ascending
9	2009/09/30	HH	Ascending	11	2017/12/26	VV	Ascending
10	2010/07/03	HH	Ascending	12	2018/01/19	VV	Ascending
11	2010/08/18	HH	Ascending	13	2018/02/24	VV	Ascending
12	2010/10/03	HH	Ascending	14	2018/03/20	VV	Ascending
13	2010/11/18	HH	Ascending	15	2018/04/13	VV	Ascending
Sentinel -1A				16	2018/05/19	VV	
1	2017/03/13	VV	Ascending	17	2018/06/12	VV	Ascending
2	2017/04/06	VV	Ascending	18	2018/07/18	VV	Ascending

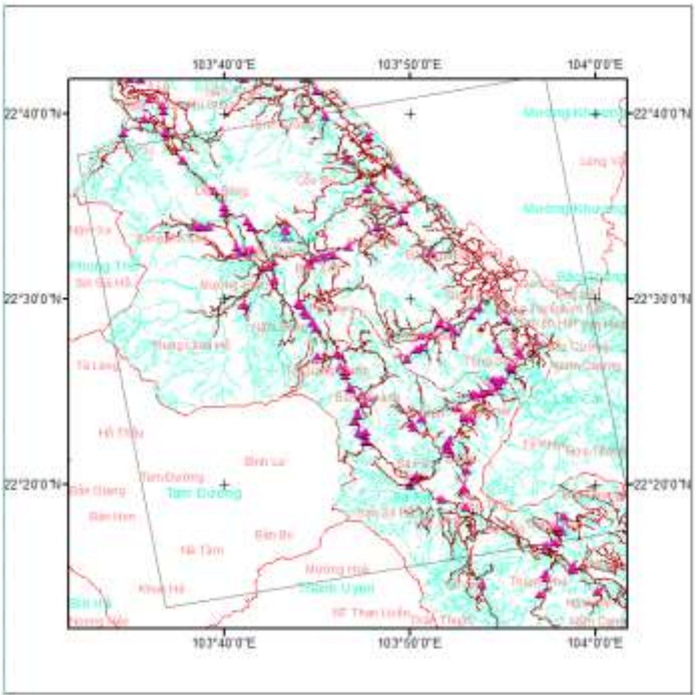

Figure 3: Survey landslide positions (magenta triangle)

In addition to the image dataset and DEM, a survey map of the landslide sites of the study area was provided by the Vietnam Institute of Geosciences and Mineral Resources . This map was surveyed in 2013 with landslide positions located mostly near traffic routes, bare lands and rivers. These points were marked with magenta triangle points and displayed on the Fig 3.

3.3 Data processing

According to the method presented above, we have applied a time-series images processing of ALOS-PalSAR-1 and Sentinel-1 images (Fig. 4)

Time series deformation was determined through the steps of the flow chart on Fig.3. Each steps in the flow chart are explained briefly:

- The SAR coregistration procedure consists of two steps: (1) First step: Coarse coregistration for pixel level accuracy, including searching for coarse image offsets and shifting the slave image; (2) Second step: Fine coregistration for subpixel accuracy, including searching for sub-pixel tie points, fitting transformation equations, and re-sampling the slave image.
- Amplitude stability index D_A is a measure of amplitude stability. It is computed as

$$D_A = 1 - \frac{\sigma_A}{m_A} \quad (8)$$

where rn_A and σ_A are the mean and the standard deviation of the amplitude values.

- Mask for sparse points selection: With this step a threshold of the Amplitude stability index value will be inputted, with values greater than the threshold to be selected and the remaining will be masked. For the case of mountain areas we have chosen a threshold value of 0.75.
- External DEM: is used to remove the topographic phase and geocoding images. In this case we use SRTM DEM 90m.
- Filtering to eliminate noise phase. We have chosen the Adaptive Goldstein filter method. This filter is one of the most well-known filters and has been widely used to improve the quality of InSAR pairs with the elimination of different types of noise.
- Estimation of spatially uncorrelated and coherence –like coefficient ξ_p : The estimation of this coefficient is mentioned above in detail. Since this coefficient will be chosen as a weight, if a weighted threshold is satisfied, it will continue to take the next step.
- Atmospheric phase screen (APS) removal: The sets of points based on reflectivity map and spatial coherence was used during the compensation of APS. Inverted residuals APS were estimated using the stratification option in order to estimate the correlation between APS and elevation DEM, compensating the vertical stratification of APS for the coherent points in different altitude over mostly mountainous area.
- After APS removal, the final estimates of deformation velocity were computed. Assuming that the deformation of each point target is d = [d1, d2, . . . dn] and the corresponding time baseline is T = [T1, T2, . . . Tn], then a weighted least square is used to calculate the deformation rate, provided that the mean square error of the interferometric phase serves as the deformation weight.

$$\upsilon = (T^T P T)^{-1} T^T P d \quad (9)$$

where υ stands for the deformation velocity, T represents the corresponding time baseline, d is time series diformation, P is the weight matrix and defined as:

$$P = diag(\sigma^1, \sigma^2, \dots \sigma^M)\sigma^k \quad (10)$$

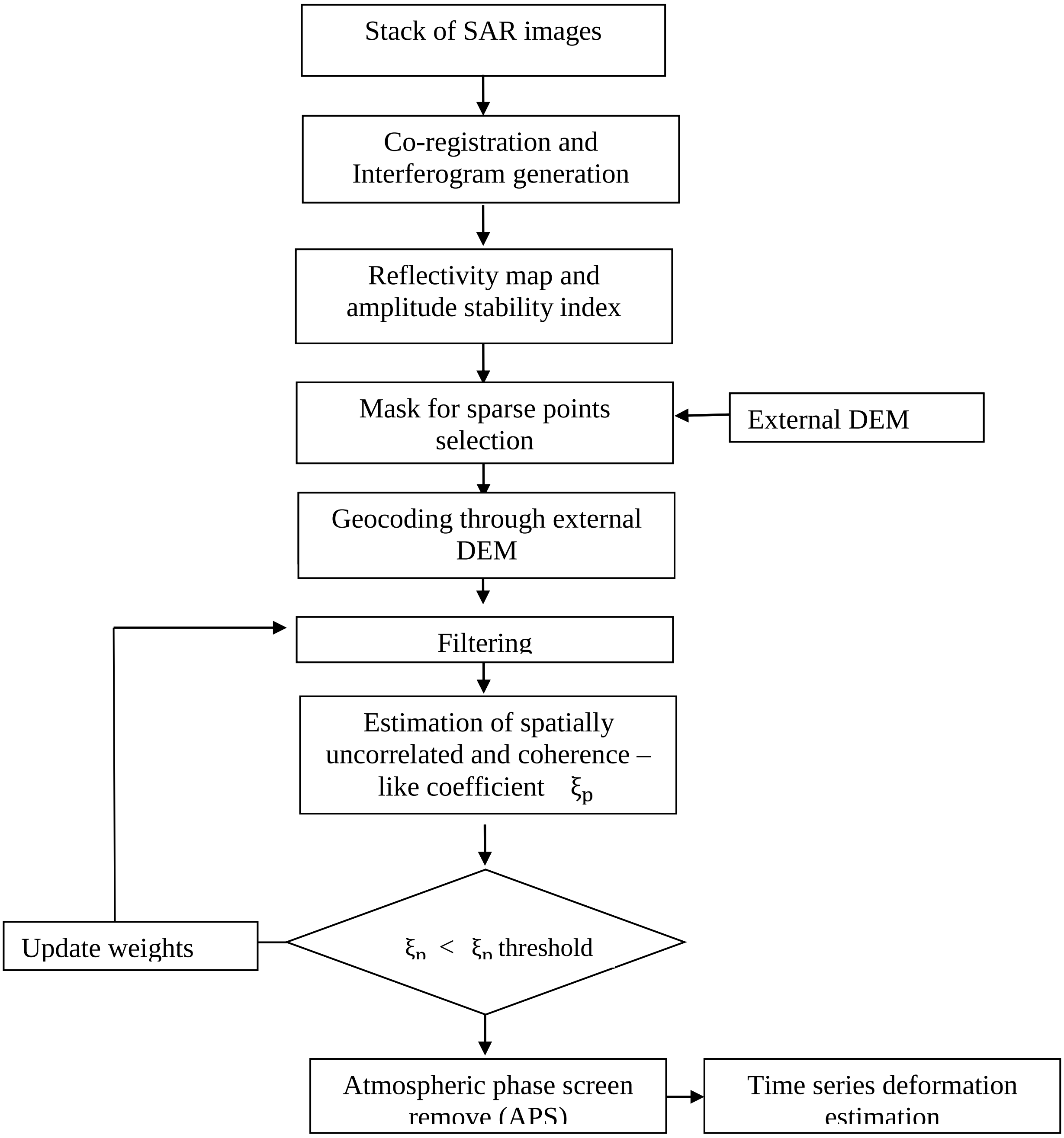

Figure 4: Flow chart of the time-series images processing

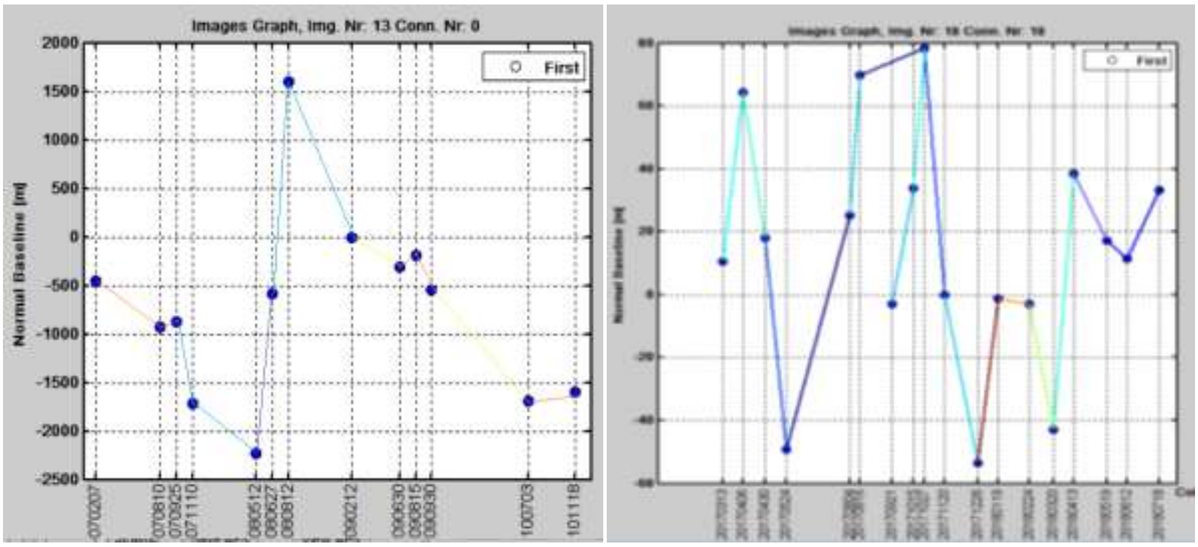

Figure 5: Chart of positions and the connection of ALOS PalSAR-1 (left), Sentinel-1A (right)

4. RESULTS AND DISCUSSIONS

After applying the Quasi-PSI method for 13 scenes of ALOS PalSAR image and 18 scenes of Sentinel -1A images of the study area by SARProz software running on Matlab 2016a (Daniel Perissin, 2009), the baselines of all pairs were obtained. Figure 5 shows the positions of image pairs and the study area was cut of 20kmx20 km on Bat Xat, Sa Pa - Lao Cai province.
In the figure 5, the vertical axis represents the distance of the baselines of the image pairs. With the terrain changed, the short baseline distance is good. There are 12 pairs of ALOS PalSAR-1 images and 17 pairs of Sentinel-1A images created with short baselines. The determination of PS and DS points is based on the threshold of Amplitude stable Index and in this case those points were chosen greater than 0.75. There are15063 PS and DS points of ALOS PalSAR and 20100 PS and DS points of Sentinel-1A that satisfy the criteria.
After removing the effects of the atmosphere by automatically downloading the orbit files and the weather of the acquisition dates, we obtained the location of the landslide rate in the period from March 2007 to November 2010 by ALOS PalSAR-1 and January 2017 to July 2018 by Sentinel-1A. Figure 6 shows the locations of landslide rate in the period 2007 -2010 were transformed into shape files and displayed in ArcGIS 10.2. Similarly, Figure 8 depicts the landslide rate over the two years 2017-2018.
For the ALOS PalSAR-1 image, Sliding points were concentrated mainly in 2 locations: Muong Hum, Densang – Batxat district and Ta Phin - Sapa town where are marked with A and B. The map of landslide survey locations in the study area provided by Vietnam Institute of Geosciences and Mineral Resources was used to overlay with landslide points from ALOS PalSAR-1 images. There were many surveying points that coincided with the landslide points from ALOS PalSAR, although the time of field survey was 2013 and different from the time of ALOS PalSAR images (Fig. 6), this proved that these positions are frequent landslides. The two positions A and B were also magnified in Fig. 7.
The sites marked as a set of points ranging from negative to positive that means they are from red to blue color dots, which confirms that landslides occur at negative sites and accumulate in positive positions. When we encounter variable sets of red, yellow, cyan and blue, these

sites will have regular landslide over time and are easily recognizable. In Fig. 7, the slide points at A were also marked in ellipses, the sliding positions were distributed near the rivers, streams and roads, the largest landslides were -350mm / year. At B position, the sliding points concentrate quite a lot in Sa Pa town which indicated by yellow dots and the slide rate value of these area was -100mm / year

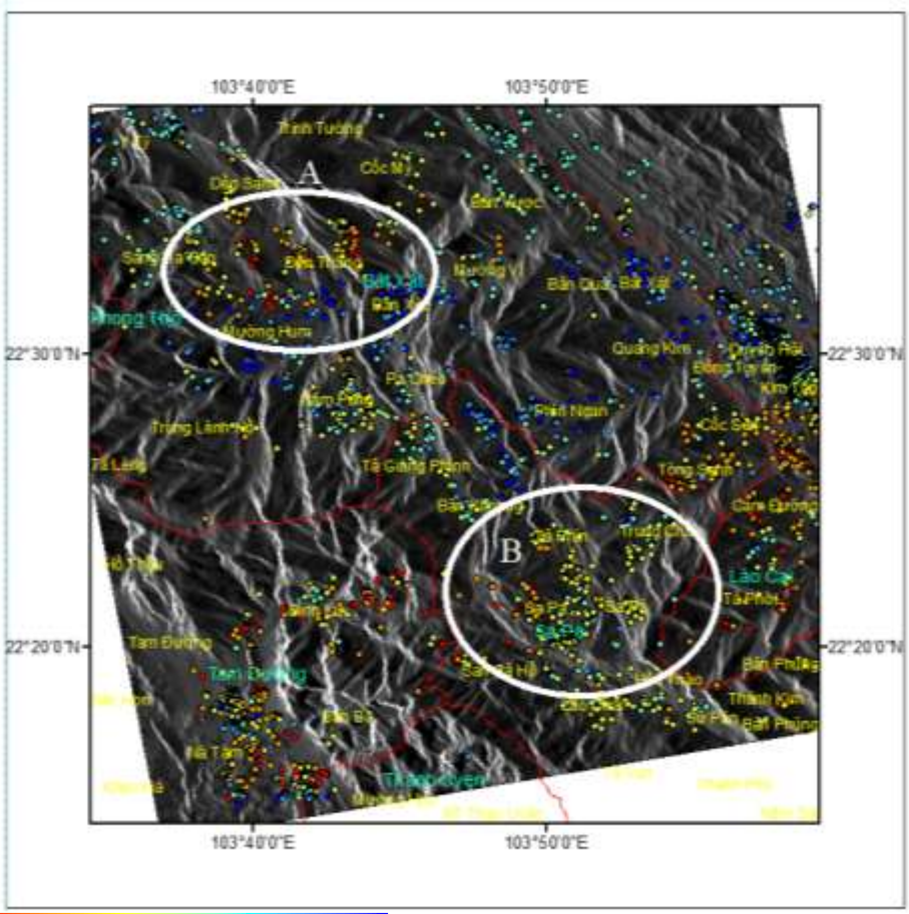

-350mm 500mm

: The boundary of districts

Figure 6: The location of the landslides were determined from the ALOS PalSAR-1 images.

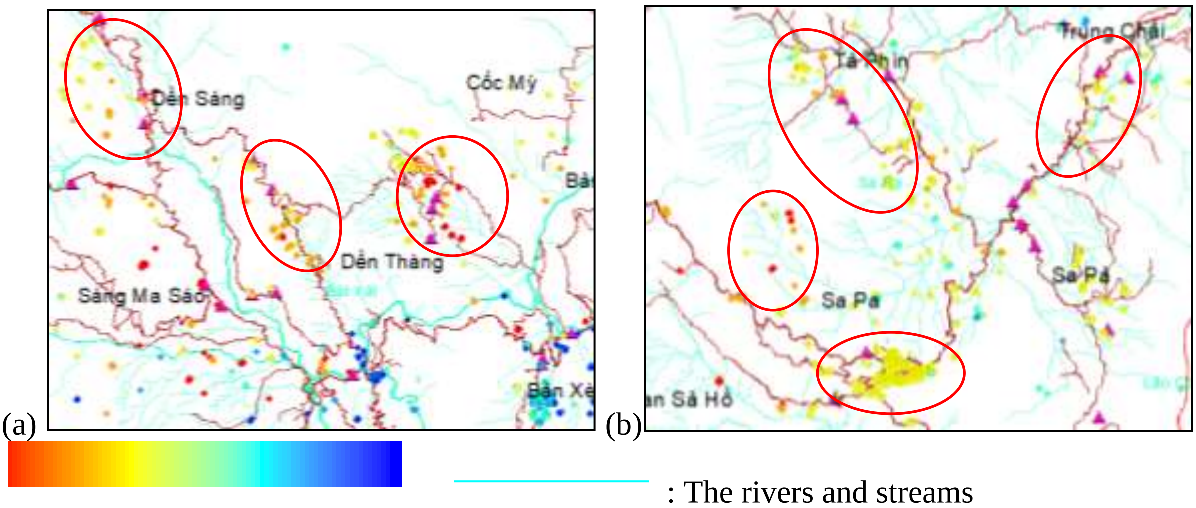

: The rivers and streams

-350mm 500mm : The surveying landsdide points

Figure 7: Landslide points by ALOS PalSAR at A and B were overlapped with survey slide points. (a): A position; (b): B position

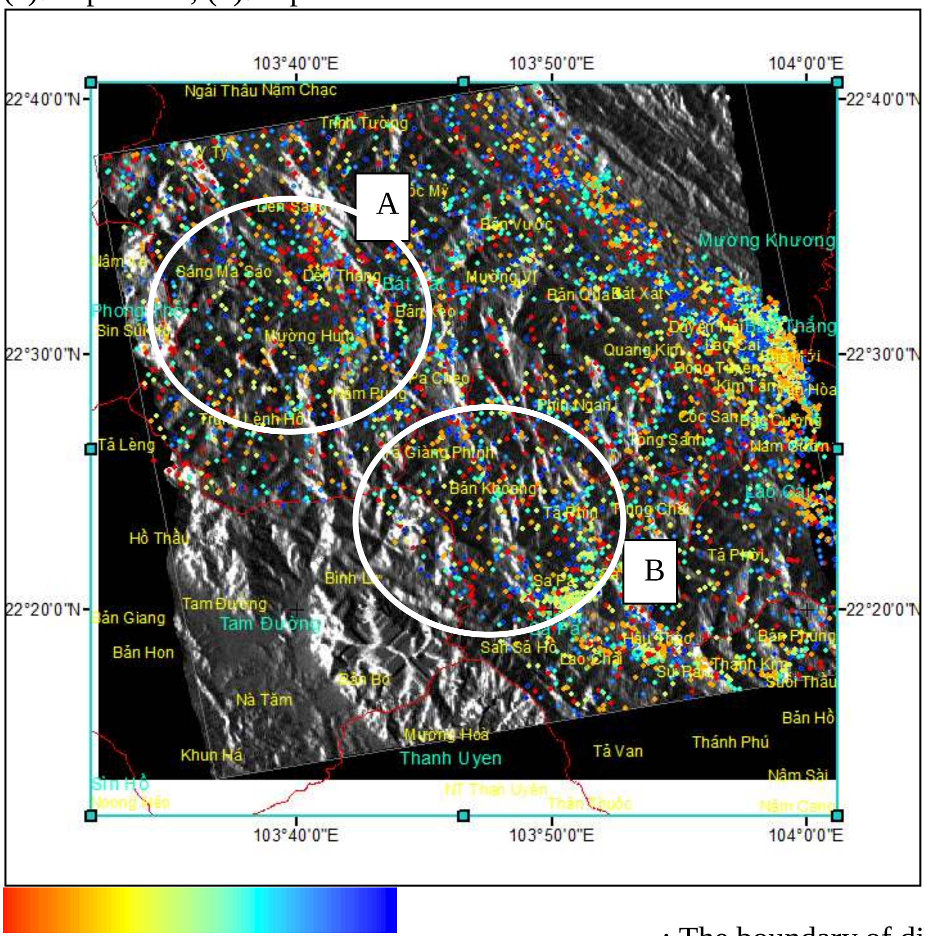

: The boundary of districts

-100mm 150mm

Figure 8: Locations of landslides determined from the Sentinel -1A images

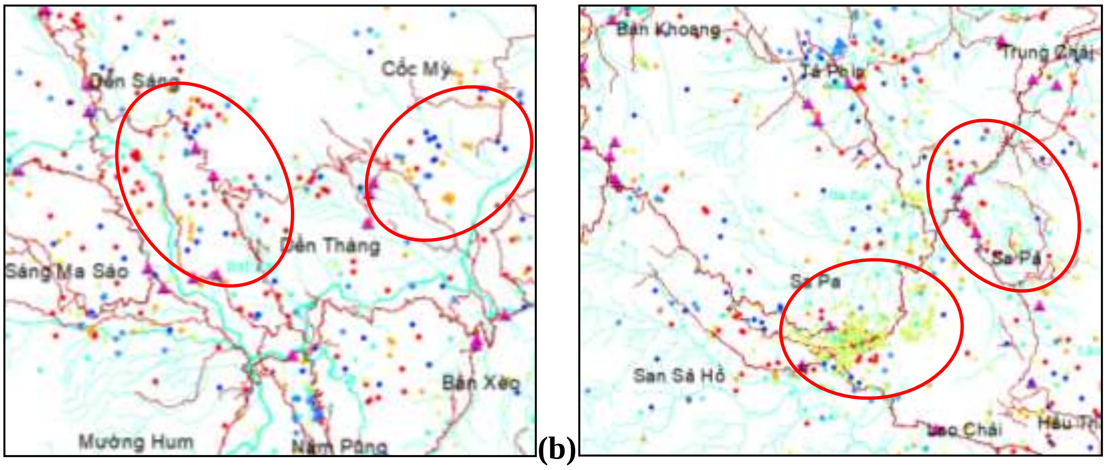

Figure 9: Locations of landslides determined from the Sentinel -1A images at A and B were overlapped with survey slide points. (a): A position; (b): B position

With the Sentinel -1A, the number of images were many more than the ALOS -PalSAR-1 image, and the correlations are higher. The number of PS and DS points was also determined. Most of the landslides were well detected for the marked locations as in the ALOS PalSAR-1 image. Figure 8 shows the slides detected from the Sentinel-1A images. At the mark's positions (A and B), the average sliding points appear almost everywhere and the maximum landslide value is -100mm / y. Beside that landslide locations made from Sentinel-1A also appear near the rivers and the roads. Fig. 9 was also magnified from Fig.8 at two positions A and B. At position A, some of the slide points coincided with the slide points on the ALOS images and there were some new landslide's spot at Den Sang or Den Thang. At position B, slide points were concentrated much in Sa Pa town as well and closed to QL4D road. There were some new slide points at Trung Chai commune and different from sliding position made from ALOS PalSAR images.

By processing two types of Radar satellite images, we found that the landsides from ALOS-PalSAR image was more coincided with the survey points than the landslides made from Sentinel-1 satellite image because the time of landslide surveying is closer to the time of ALOS PalSAR acquisitions than Sentinel-1A. However, there were some landslide points where both types of images could be detected at the same places, which were susceptible to landslides that remain in these places from 2007 to 2018. These slide points were massed in Densang- Batxat district and Sapa town where is near QL4D road

5. CONCLUSION

With the set of 13 ALOS –PalSAR images and 18 Sentinel-1A images which were subsetted in about 20kmx20km, we processed these scenes using the Quasi-PSI method using Saproz software running on Matlab 2016a. The landslide identification results indicate the following:

The Quasi-PSI method is suitable for mountainous areas with dense vegetation cover due to the selection of optimal coherence values and used them as weight to eliminate unsatisfactory PS points.

The ALOS PalSAR-1 images was used for over 3 years from 2007 to 2010, while the Sentinel-1 images was used for one and half years from the beginning of 2017 to the middle of 2018. With ALOS palSAR dataset, the baselines were a bit long, besides, coherence of the image pairs were not high, thus the number of PS and DS points were not much, only 15063 points. With the higher number of images and the shorter baselines, the correlation of the image pairs was also higher so the number of PS and DS points was 20100 points. These points were the points used to determine landslides.

Landslide survey sites provided by the Vietnam Institute of Geosciences and Mineral Resources were collected in 2013, which was different from the two time series of images. However, this time was close to ALOS palsAR image so there were a lot of sliding positions coinciding with the sliding position determined from the ALOS PalSAR images. For Sentinel-1 images, the time of acquiring images were quite far from the time of survey so the sliding positions were different. There was the locations in Densang and Sapa town where near the QL4D road were always at risk of sliding because it existed from 2007 to 2018. Since then, determining of the landslides from Radar satellite images can be used to detect at large, frequent and long-term landslides.

Due to the landslide identification from the radar image is possible to get the sliding rate whereas the survey landslide is not available, therefore it is only possible to determine the location of landslide that occurred for comparing. In the near future we are planning to attach sensors to measure the sliding speed in some susceptible landslide locations to compare with the method of using radar interferometry method.

ACKNOWLEDGMENTS

We sincerely thank Dr. Daniel Perissin of Purdue University, author of the Saproz software, helped and commented on the Sentinel-1A data processing.

REFERENCES

Bruckno Brian, Vaccari Andrea, Hoppe Edward, Nieaman Wiliam, Campbell Elizasbeth, 2013, *Validation of Interferometric Synthetic Aperture Radar as a Tool for Identification of Geohazards and At-Risk Transportation Infrastructure*. Paper in the Earth and Atmospheric Sciences. 402 University of Nebraska-Lincoln.

Berardino, P., Fornaro, G., Lanari, R. & Sansosti, E. 2002. A New Algorithm for Surface Deformation Monitoring based on Small Baseline Differential SAR interferograms, IEEE TGARS, vol. 40, no. 11, pp. 2375-2383.

D. Perissin and T. Wang, Repeat-Pass SAR Interferometry With Partially Coherent Targets, 2012. *IEEE Transactions on Geoscience and Remote Sensing*, vol. 50, no. 1, pp. 271-280

Daniele Perissin, 2009. Sarproz Manual, https://www.sarproz.com/software-manual/

Engelbrecht J., 2016. *Differential radar interferometry for deformation monitoring*. Link http://www.ee.co.za/article/differential-radar-interferometry-deformation-monitoring.html Public May 9th, 2016, Accessed Oct 10th, 2017

Ferretti, A., Prati, C. and Rocca, F., 2000. Nonlinear subsidence rate estimation using permanent scatters in differential SAR interferometry, *IEEE Transactions on Geoscience and Remote Sensing*, **38**(5), pp. 2202-2212.

Gabriel and Goldstein, 1989. Mapping small elevation changes over large areas: Differential ra-đa interferometry, Journal of Geophysical Research, vol. 94(B), no. 7, pp. 9183-9191.

Herrera, G., Tómas, R., Monells, D., Centolanza, G., Mallorquí, J.J., Vicente, F., Navarro, V.D., Lopez-Sanchez, J.M., Sanabria, M., Cano, M., Mulas, J., 2010. Analysis of subsidence using TerraSAR-X data: Murcia case study. Eng. Geol. 116, 284-295.

Hooper, A., H. Zebker, P. Segall, and B. Kampes, 2004. A new method for measuring deformation on volcanoes and other natural terrains using InSAR persistent scatterers, Geophys. Res. Lett., 31.

Javier Hervas, Jose I. B., Paul L.R., 2003. Monitoring Landslide from optical remotely sensed imagery: the case history of Tessina landslide, Italy,.Geomorphology 54, 63-75

Kim Jin-Woo, ZhongLuandKimberlyDegrandpre, 2016. *On going Deformation of Sinkholes in Wink,Texas, Observed by Time-Series Sentinel-1A SAR Interferometry (PreliminaryResults).* Remote Sens. 2016, 8, 313; doi:10.3390/rs8040313

Le Ba Thao (2009). Nature of Vietnam . Education publisher, 324p

Massonnet D., M. Rossi, C. Carmona, F. Adragna, G. Peltzer, K. Feigi and T. Rabaute, 1993. The Displacement field of thelander earthquake mapped by radar interferometry. Nature, 364, pp.138-142

McKean, J., Buuechel, S., Gaydos, L., 1991. Remote sensing and landslide hazard assessment. Photogrammetric Engineering and Remote Sensing 57 (9), 1185-1193

Ran N. Nof, Gidon Baer, Alon Ziv, Eli Raz, Simone Atzori, Stefano Salvi, 2013. *Sinkhole precursors along the Dead Sea, Israel, revealed by SAR interferometry*.Geological Society of America DOI: 10.1130/G34505.1 Published on July 2013, First Published on July 03, 2013

Refice A., Convenga F., Nutricato R., 2003. Stepwise approach to InSAR processing of multitemporal datasets, Proc. of Fringe 2003

Soeters, R., van Westen, C.J., 1996. Slope instability recognition, analysis and zonation. In: Turner, A.K., Schuster, R.L. (Eds.), Landslide Investigation and Mitigation: National Research Council, Transportation Research Board Special Report vol. 247, pp. 129-177.

Theron A., Engelbrecht, J. and Kemp, J. 2016. Potential of sinkhole precursor detection through interferometric SAR. Conference Paper, Aug 2016.

Van Anh Tran, Quoc Cuong Tran, Duc Anh Nguyen, Tong Minh Dinh Ho, Trung Anh Tran, Nhu Hung Nguyen, 2016, Application of PSInSAR method for determining of land subsidence in Hanoi city by Cosmo-Skymed imagery, proceeding in GIS-IDEAS conference 2016

BIOGRAPHICAL NOTES

CONTACTS

Name: Van Anh Tran
Institution: Faculty of Geomatics and Land Administration, Hanoi University of Mining and Geology, Vietnam
Address: 18 Vien street, Duc Thang ward, Bac Tu Liem District
City: Hanoi
COUNTRY: Vietnam
Tel. +84986811971
Email:vananhtdavt@gmail.com